

# CCD Camera Array System for Electron Density and Temperature Measurement in the LHD Plasma Periphery

SHOJI Mamoru, YAMAZAKI Kozo, ICHIMOTO Shinji and LHD Experimental Group  
National Institute for Fusion Science, Toki 509-5292, Japan

(Received: 11 December 2001 / Accepted: 5 July 2002)

## Abstract

An image data analysis system using four CCD cameras has been developed for measuring electron density and temperature profiles on divertor legs. The image data are analyzed by image processing software after every plasma discharge. The system was installed in a tangential port, and applied to measurement after the calibration of the CCD sensitivity of each camera. While the electron density on the divertor leg increased with the main plasma density, the decrease of the electron temperature on the divertor leg was observed. These dependencies on the main plasma density agree with the experimental data by a fast moving Langmuir probe and probes embedded in divertor tiles, indicating the availability of the CCD camera array system for plasma parameter measurements on the divertor leg.

## Keywords:

CCD camera, HeI intensity ratios, divertor leg, image processing, Large Helical Device

## 1. Introduction

Large Helical Device (LHD) consists of two helically twisted magnetic coils and three pairs of circular poloidal coils. Three dimensionally complicated peripheral plasmas (ergodic layer and divertor legs) are formed by the magnetic coils. The measurement of the plasma parameters on the divertor legs with visible CCD cameras is useful for complicated shaped plasmas such as LHD plasmas because of the high spatial resolution, wide viewing areas and simple instrumental configurations. It has been found that the electron density and temperature in the plasma periphery can quantitatively be measured by HeI line intensity ratios [1]. Conventionally, the HeI line intensity ratios have been measured by spectroscopes. Many spectroscopes, thus, are necessary to measure the plasma parameter profiles. For observing simply the plasma parameter profiles, we have developed CCD camera array system in order to measure the images of the line intensity ratios using an image capture board and image

processing software.

The calculations by tracing the magnetic field lines with a random walk process from the ergodic layer predict that the distribution of the particle deposition pattern on divertor plates is three-dimensionally complicated. Thus, the CCD camera array system can be a useful device for measuring three dimensionally complicated profiles of the plasma parameters on the divertor leg which can not be measured by Langmuir probes (0-dimensional measurement).

## 2. CCD Camera Array System for Measuring Plasma Parameter Profiles

In order to measure the profile of the HeI line intensity ratios, three interference filters (center transmit wavelength  $\lambda_0 = 668.8$  nm, 707.7 nm and 728.4 nm, respectively) are mounted at the front of the cameras [2]. We used the cameras (SONY: DXC-LS1) with a separated small CCD head ( $\phi 12 \times 60$  mm). By

---

Corresponding author's e-mail: [shoji@LHD.nifs.ac.jp](mailto:shoji@LHD.nifs.ac.jp)

mounting the CCD heads side by side at a tangential port (7-T), we can actually neglect the difference of the position of the cameras, because the distance between each camera ( $\sim 14$  mm) is much smaller than the distance between the cameras and the peripheral plasma ( $\sim 2.8$  m). The gain and shutter speed can remotely be controlled from the LHD control room. The HeI line intensity ( $\lambda = 728.1$  nm) is much weaker than the other two HeI line intensity ( $\lambda = 667.8$  and  $706.5$  nm) [3]. Thus, we have observed the background intensity by another camera with the interference filter which central transmit wavelength is  $720.6$  nm. We regard the exact HeI intensity ( $\lambda = 728.1$  nm) as that which is reduced by the background intensity. For applying interference filters to cameras, it should be noted that the central transmit wavelength of the filter is shifted to the lower wavelength side when the incident angle of light to the filters is not  $0$  degree, which is expressed as the following formula [4]:

$$\lambda_{\alpha} = \lambda_0 \sqrt{1 - \left(\frac{N_e}{N^*}\right)^2 \sin^2 \alpha}, \quad (1)$$

where  $\lambda_0$  is the center transmitted wavelength at normal incidence,  $N_e$  is refractive index of the external medium (air:  $N_e = 1.0$ ),  $N^*$  is that of the interference filter ( $\sim 1.5$ ), and  $\alpha$  is the incident angle of light. In our camera system, the maximum incident angle of light from the peripheral plasma is less than  $5$  degrees, thus, the maximum shift of wave length due to the finite incident angle is estimated to be about  $1.0$  nm. Therefore, we used relatively wide band pass filters ( $\lambda_{1/2} \sim 5.0$  nm) so as to reduce the wavelength shift effect. Here, the parameter  $\lambda_{1/2}$  means the full width of the half maximum (FWHM) wavelength of the transmittance. A demerit of using wide band pass filters is that some line emission except the HeI lines can be mixed into the transmitted light. We confirmed that no prominent line emission near the wavelength of the three HeI lines exist by a visible spectroscope. Bremsstrahlung is another possible obstacle for the measurement, experimental results with the spectroscope show that the intensity by Bremsstrahlung is much smaller than the two HeI lines ( $\lambda = 667.8$ ,  $706.5$  nm) in standard plasma discharges with He gas fueling. The effect of Bremsstrahlung on another weak HeI line ( $\lambda = 728.1$  nm) can be reduced by using the background light intensity ( $\lambda_0 = 720.6$  nm).

The images of the HeI line emission and background light taken by the CCD cameras are combined into an image by a video multiplexer. The image is transferred to the control room via an optical

fiber. The data are captured and saved in memories mounted on an image capture board (Microtechnica: MTPIC-CD).

### 3. Calibration Experiment for the CCD Cameras

Before applying the camera system to plasma measurement, we had determined the relative sensitivity of the cameras by using a tungsten lump. The relative sensitivity of the camera  $S$  is defined by the following formula:

$$S = \frac{A}{L \cdot T_{\max} \cdot \lambda_{1/2}}, \quad (2)$$

where,  $L$  ( $\text{W} \cdot \text{cm}^{-3} \cdot \text{str}^{-1}$ ) is the emissivity of light from the tungsten lump at the center transmit wavelength of each interference filter, and  $T_{\max}$  (%) is the maximum transmittance of the interference filter. We determined the parameter  $A$  by measuring the dependence of the intensity of the tungsten filament on the accumulated light. Figure 1 gives the dependence of the average intensity on the image of the filament. We controlled the accumulation of light by using neutral density (ND) filters ( $T = 50, 32, 10$  %) and by changing the exposure time of the cameras ( $\Delta t = 500, 250, 125, 100$   $\mu\text{s}$ ). The parameters  $T$  and  $\Delta t$  mean the transmittance of the ND filters mounted in front of the camera, and the exposure time, respectively. It is generally known that the intensity from cameras saturates when a measured object is

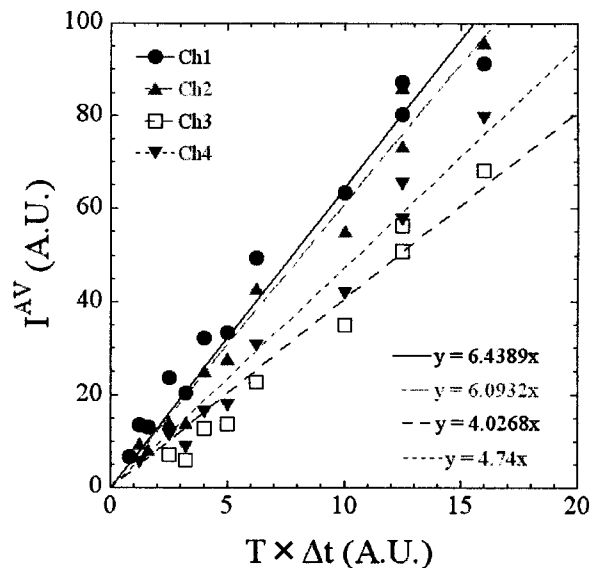


Fig. 1 Dependence of the average intensity of the tungsten filament on the accumulated light.

too bright. We controlled the exposure time so as not to exceed the intensity over about 100 (A.U.) in plasma measurement. The parameter  $A$  was deduced from the least mean square fitting of the intensity plots. Using the formula (2), we determined the relative sensitivity of each camera as follows:

$$S_{Ch1}(668.8 \text{ nm}): 1.0000, S_{Ch2}(707.7 \text{ nm}): 0.7368, \\ S_{Ch3}(728.4 \text{ nm}): 0.4796, S_{Ch3}(720.6 \text{ nm}): 0.5490.$$

By dividing the measured intensity by the relative sensitivity, we can obtain the relative intensity of the HeI lines and background light.

For measuring the plasma parameter profiles with the cameras, the uniformity of the sensitivity of pixels on CCD is important. We confirmed the uniformity in the practical area on CCD by changing the position of the tungsten lump and by measuring the intensity profile with a light diffuser plate for flat-field measurement.

#### 4. Analysis of Image Data Taken by the CCD Cameras

The captured images are divided into four images by the software (Planetron: Image-Pro Plus) so as to get the calibrated intensity profile of each HeI line and the background light. The images are transformed into a standard formatted image to cancel the difference of the viewing angle of each camera, enabling direct comparison of the intensity profiles. The electron density and temperature are derived from the following formula:

$$n_e : \frac{\alpha I_{Ch1}}{I_{Ch3} - I_{Ch4}}, \quad T_e : \frac{\beta(I_{Ch3} - I_{Ch4})}{I_{Ch2}}, \quad (3)$$

where,  $I_{ChN}$  expresses the calibrated intensity of the image taken by the camera (channel  $N$  ( $N = 1 \sim 4$ )) on a pixel. The parameters  $\alpha$  and  $\beta$  mean calibration factors for converting the HeI intensity ratios to the electron density and temperature, respectively. We determined the calibration factors from the ref. [1] using typical plasma parameters in the LHD divertor plasma (the electron density and temperature are  $5 \times 10^{18} \text{ m}^{-3}$  and 50 eV, respectively).

#### 5. Measurement of the Plasma Parameters on the Divertor Leg

From view ports (except for tangential ports), the light from the divertor legs is unclear, because the main plasma disturbs optical measurement of the divertor legs. We, thus, installed the camera system at a tangential port. Figure 2 illustrates the CAD image showing typical LHD plasma from the tangential port,

which indicates that the image of the divertor leg inside the divertor region is emphasized by the line integration. Figure 3 shows a raw HeI line intensity images in an NBI heated plasma with He gas fueling in which the average main plasma density gradually increases. We observed the images by controlling the exposure time of each camera (Ch1:  $\Delta t = 17 \text{ ms}$ , Ch2: 50 ms, Ch3: 250 ms, Ch4: 250 ms) so as to maximize the measured intensity on the divertor leg within the linear response range of the intensity (see Fig. 1). Figure 4 and 5 illustrate the time evolution (1.1 s and 1.7 s) of the

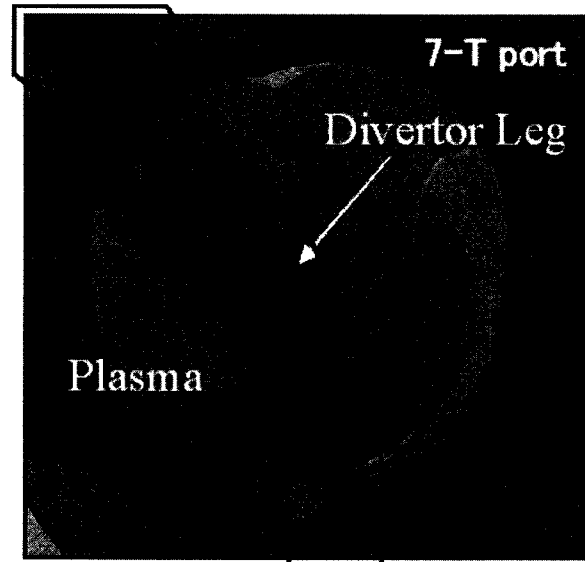


Fig. 2 CAD image of the LHD plasma and the divertor leg from a tangential port (7-T).

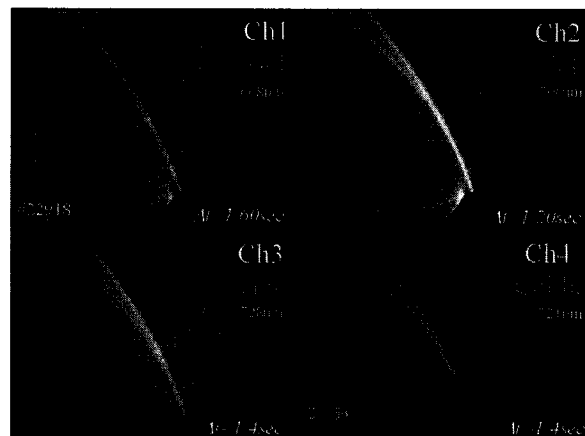


Fig. 3 Raw image taken by the CCD camera array system in an NBI heated plasma with He gas fueling.

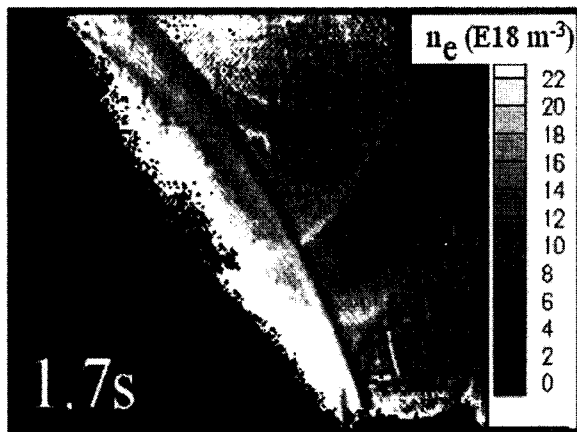
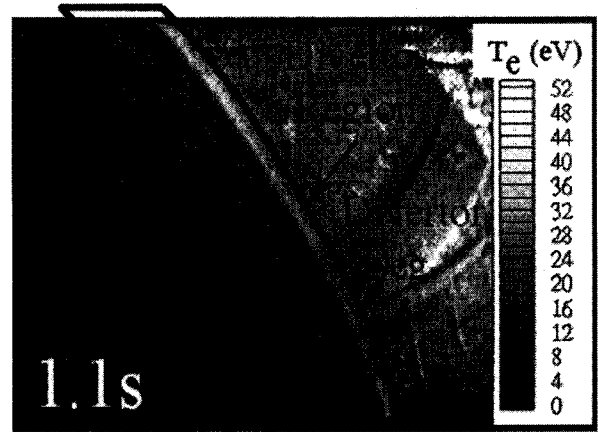
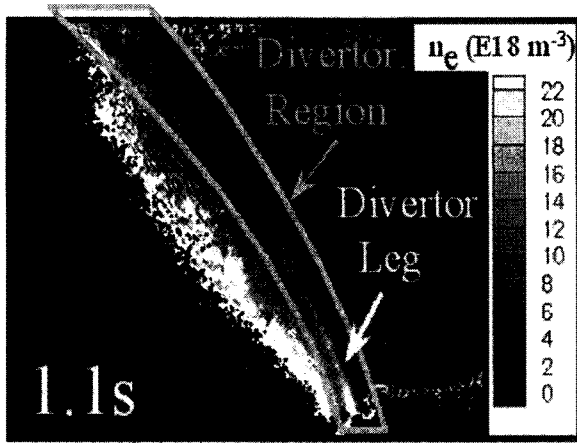


Fig. 4 Time evolution of the electron density profile on the divertor leg measured by the CCD camera array system.

Fig. 5 Time evolution of the electron temperature profile on the divertor leg measured by the CCD camera array system.

electron density and temperature image after image processing, respectively. The area enclosed by a gray and a black line in these figures corresponds to the divertor region. Considering the CAD image shown in Figure 2, we think that the upper region inside the divertor region is appropriate to estimate the plasma parameters on the divertor leg. This is because the length of the line of sight being across the divertor leg in the region is longer than that in the other region. The electron density on the divertor leg rises from  $\sim 3 \times 10^{18} \text{ m}^{-3}$  at 1.1 s to  $\sim 8 \times 10^{18} \text{ m}^{-3}$  at 1.7 s with the average main plasma density (from  $\sim 2 \times 10^{19} \text{ m}^{-3}$  at  $t = 1.1 \text{ s}$  to  $\sim 4 \times 10^{19} \text{ m}^{-3}$  at 1.7 s), while the electron temperature on the divertor leg decreases from  $\sim 45 \text{ eV}$  at 1.1 s to  $\sim 24 \text{ eV}$  at 1.7 s. The measurements of plasma parameters on the divertor leg and these dependencies on the main plasma density are qualitatively consistent with the

measurements of Langmuir probe embedded in divertor plates. The measurements show that the divertor plasma density rises with the main plasma density and the electron temperature gradually decreases with the main plasma density [5], indicating the availability of the camera array system for the plasma parameter measurement on the divertor legs.

Next, we discuss possible experimental errors in our camera system. It can be listed as follows:

1. the wavelength shift effect by the finite incident angle of the emission,
2. the finite difference between the center wavelengths of transmittance of the interference filters and these of the observed HeI lines,
3. the ambiguity of the relative sensitivities of the CCD cameras,
4. the instrumental uncertainty for acquiring and digitizing the output signal from the cameras,

5. the conversion error of the HeI line intensity ratios to the plasma parameters ( $n_e$  and  $T_e$ ).

The first and second experimental errors can cause the less than 8 % reduction of the intensity of the HeI lines, leading to the about 10 % reduction and rise of the  $n_e$  and  $T_e$ , respectively. We estimated about 10 % error of the plasma parameters due to the third and fourth experimental errors from the intensity plots of the cameras in the calibration experiment in the intensity range (> 60 A.U.) which was actually used in plasma measurement. The fifth conversion error definitely determines the accuracy of the plasma parameters in our camera system. The data to convert the HeI line intensity ratios to the plasma parameters was derived under some idealized theoretical assumptions (no high energy electrons, and no He<sup>+</sup> recombination, etc.). Considering the theoretical assumptions and the ambiguity of the dependence of the intensity ratios on the plasma parameters, we estimated the overall measurement error to be a factor of about 2.5

in  $n_e$  measurement and about 40 % in  $T_e$  measurement on the divertor legs, respectively. The reason why the experimental error for the electron temperature is smaller than that for the electron density is ascribed to the significant variation of the HeI line intensity ratios to the change of the electron temperature in typical plasma parameters on the LHD divertor legs.

#### References

- [1] B. Schweer *et al.*, J. Nucl. Mater. **196-198**, 174 (1992).
- [2] M. Shoji *et al.*, J. Plasma Fusion Res. SERIES 3, 440 (2000).
- [3] E de la Cal *et al.*, Nucl. Instrum. And Methods **A403**, 490 (1998).
- [4] F. Meo *et al.*, Rev. Sci. Instrum. **68**, 3426 (1997).
- [5] S. Masuzaki *et al.*, J. Nucl. Mater. **290-293**, 12 (2001).